A Calcium−Metalloribozyme with Autodecapping and Pyrophosphatase Activities†

Faqing Huang and Michael Yarus*

Department of Molecular, Cellular, and Developmental Biology, University of Colorado at Boulder, Boulder, Colorado 80309-0347

Received May 8, 1997; Revised Manuscript Received July 30, 1997⊗

ABSTRACT: A previously-isolated ribozyme with capping activity has self-decapping activity, here characterized alongside its additional, somewhat parallel, pyrophosphatase reaction. Decapping is 10−50 times slower than the pyrophosphatase activity, depending on pH. The RNA accelerates pyrophosphate release 170 000 times over a control composed of randomized pppRNA, and 5′ capped RNA accelerates decapping 1000-fold over random capped RNA. Triphosphate-linked G(5′)pppRNA also supports an unusual cap-exchange reaction, exchanging its cap with guanosine 5′-tetraphosphate to form pentaphosphate-linked G(5′)ppppRNA. GDP, a capping reactant for the RNA, appears to suppress both decapping and pyrophosphatase activities. Autodecapping and pyrophosphatase activities have in common an unusual divalent metal ion requirement for Ca^{2+} or less effectively Mn^{2+}, and both are active over a broad pH range of 4.5−9.0. These characteristics resemble the capping activity of the same RNA. Kinetic analysis reveals a well-defined Ca^{2+}−RNA complex, and Mg^{2+} and Sr^{2+} act as competitive inhibitors of Ca^{2+}. A strong Ca^{2+}-binding site is suggested by a low K_M of 40−60 μM at pH ≥ 7.0. The role of Ca^{2+} in these reactions can be surmized from literature data on reactivity of nucleotide phosphates. Pyrophosphatase, capping, and decapping activities of isolate 6 RNA are apparently carried out by a single reaction center, whose rate of reaction with all nucleophiles sums to a constant total rate. This suggests a universal rate-limiting step. Versatile activation of α-phosphate by this reaction center raises the possibility of combinatorial ribozymes.

Decapping of eukaryotic mRNA is essential for normal rates of mRNA turnover (Beelman et al., 1996). By virtue of controlled degradation of capped mRNA, decapping is, in effect, one of the strategies that regulate protein synthesis. In cells, decapping of eukaryotic mRNA is carried out by protein-decapping enzymes (Stevens, 1980; Beelman et al., 1996). Capped mRNA is not susceptible to digestion by 5′ → 3′ nucleases. However, upon decapping, the exposed 5′ end subjects the mRNA to 5′ → 3′ exonucleolytic hydrolysis, one of the major pathways of mRNA degradation. This mRNA degradation pathway is initiated by shortening the poly(A) tail and followed by decapping and 5′ → 3′ exonucleolytic digestion (Decker & Parker, 1993, 1994; Muhlrad et al., 1994, 1995).

A self-capping catalytic RNA (104mer isolate 6; Huang & Yarus, 1997a), whose product can be a 5′ terminus like the eukaryotic mRNA cap, also acts as a versatile phosphoryl linker that can link to almost any nucleophile containing a terminal phosphate, including nucleotides, coenzymes, amino acids, sugars, and other macromolecular RNAs (Huang & Yarus, 1997b). The general reaction mechanism involves nucleophilic attack on the 5′ α-phosphate of the pppRNA (5′ triphosphate RNA) by a nonbridging oxygen of the terminal phosphate of nucleophiles, with concomitant release of PP_i:

$$\text{R-}\mathbf{p}\text{(nucleophile)} + \text{pppRNA (isolate 6)} \rightarrow \text{R-}\mathbf{p}\text{pRNA} + PP_i \quad (1)$$

Phosphoryl coupling with isolate 6 pppRNA provides a potential route for specific RNA linkage to a large variety of terminal phosphate-containing nucleophiles, including many metabolically important molecules (Huang & Yarus, 1997b). This RNA activity suggests that varied functional groups might have been recruited to the 5′ terminus of RNA to further increase RNA catalytic versatility, supporting an RNA-based metabolism pre-existing the emergence of coded protein synthesis (White, 1976; Gilbert, 1986; Joyce, 1989; Huang & Yarus, 1997a & 1997b).

In addition to phosphoryl coupling, isolate 6 pppRNA also possesses a 5′ pyrophosphatase activity (Huang & Yarus, 1997a), which releases the 5′ pyrophosphate of the pppRNA with water as attacking nucleophile:

$$H_2O\text{ (nucleophile)} + \text{pp}\mathbf{p}\text{RNA (isolate 6)} \rightarrow \mathbf{p}\text{RNA} + PP_i \quad (2)$$

We now show that 5′-capped isolate 6 G(5′)pppRNA also has a self-decapping activity, an activity similar to that of a protein decapping enzyme:

$$\text{G(5′)pp}\mathbf{p}\text{RNA (isolate 6)} \rightarrow \mathbf{p}\text{RNA} + \text{GDP} \quad (3)$$

Moreover, the decapping activity is sensitive to pH, Ca^{2+}, or GDP concentrations.

Both decapping and pyrophosphatase activities of isolate 6 RNA are characterized kinetically below, with the goal of making this reactive RNA more useful.

MATERIALS AND METHODS

Preparation of 5′ [γ-^{32}P]-Labeled Random and Isolate 6 RNAs. 5′[γ-^{32}P]-Labeled random 104mer *pppRNA (the asterisk indicates the position of ^{32}P) was prepared by transcription of random PCR DNA template from the initial

† This work was supported by NIH Grants GM30881 and GM48080 to M.Y. and an NIH postdoctoral fellowship (NRSA) to F.H.

* To whom correspondence should be addressed.

⊗ Abstract published in *Advance ACS Abstracts,* November 1, 1997.

S0006-2960(97)01081-7 CCC: $14.00

selection cycle (Huang & Yarus, 1997a) in the presence of 1 μM [γ-^{32}P]GTP. The random *pppRNA was purified by 8% denaturing PAGE (xylene cyanol = 46 cm), eluted, EtOH-precipitated, resuspended in water, and stored at −20 °C until use. 5′[γ-^{32}P]-Labeled isolate 6 *pppRNA was prepared and gel purified to single nucleotide resolution as described (Huang & Yarus, 1997a, 1997b).

*Preparation of 5′ [γ-^{32}P]-Labeled Random and Isolate 6 Capped G(5′) *pppRNA.* Unlabeled random and isolated 6 pppRNAs (both 104mers) were transcribed from DNA templates and purified by 8% denaturing gel electrophoresis as described (Huang & Yarus, 1997a). 5′[γ-^{32}P]-Labeled random and isolate 6 capped G(5′)*pppRNAs were prepared by incubating (10 μL total volume) 5 μM of unlabeled pppRNAs with 1.7 μM 5′[α-^{32}P]-GTP (3000 mCi/mmol) and 0.34 units/μL GTP:RNA guanylyltransferase (GIBCO BRL) for 1 h at 37 °C in a buffer containing 0.1 M HEPES (pH 7.5), 1 mM $MgCl_2$, 60 mM NaCl, 6 mM KCl, 2 mM DTT, and 3 ng/μL of BSA. The ^{32}P-labeled G(5′)*pppRNAs were purifed by 8% denaturing PAGE (xylene cyanol = 30 cm) and recovered as above.

Preparation of Internally Labeled Isolate 6 Capped G(5′)-pppRNA. Internally ^{32}P-labeled isolate 6 capped G(5′)-pppRNA was prepared by self-capping of internally ^{32}P-labeled isolate 6 pppRNA (gel purified to single nucleotide resolution) (Huang & Yarus, 1997a, 1997b) under the following conditions: 1 h at 37 °C; 1 μM pppRNA, 1 mM GDP, 20 mM $CaCl_2$, and 20 mM MES, pH 5.5. The resulting 5′-capped RNA was purified by 8% PAGE to single nucleotide resolution (xylene cyanol = 46 cm) and recovered as above.

*Identification of Decapping Product of Isolate 6 G(5′)*ppp-RNA.* Isolate 6 G(5′)*pppRNA (5 nM) was incubated for 3 h at 37 °C in 2 mM $CaCl_2$, 20 mM MES, pH 5.5. The reaction mixtures were resolved alongside chromatographic standards *P_i and [α-^{32}P]nucleotides, GMP (*pG), GDP (p*pG), and GTP (pp*pG) on a cellulose PEI TLC plate with 20% methanol and 80% 0.5 M potassium phosphate at pH 6.3. The standards *pG and p*pG were prepared by heating pp*pG in water for 2 h at 95 °C. ^{32}P was visualized by phosphorimaging (BioRad GS525).

Divalent Metal Ion Requirement for Decapping and Pyrophosphatase Activities of Isolate 6 RNA. Internally labeled isolate 6 G(5′)pppRNA (5 nM) was incubated for 3 h at 37 °C in different solutions (20 mM MES, pH 5.5) containing one or two different divalent metal ions: Mg^{2+}, Ca^{2+}, Sr^{2+}, Ba^{2+}, Mn^{2+}, Co^{2+}, Ni^{2+}, Cu^{2+}, and Zn^{2+}. The decapping product was separated from the reactant G(5′)-pppRNA by 8% denaturing PAGE (xylene cyanol = 46 cm) and visualized by a phosphorimager.

Isolate 6 *pppRNA (0.1 μM) was incubated for 30 min at 37 °C in 20 mM MES (pH 5.5) containing 10 mM of one divalent or trivalent metal ion: Mg^{2+}, Ca^{2+}, Sr^{2+}, Ba^{2+}, Mn^{2+}, Co^{2+}, Ni^{2+}, Cu^{2+}, Zn^{2+}, Cd^{2+}, Pb^{2+}, La^{3+}, Ce^{3+}, Sm^{3+}, and Dy^{3+}. Spermidine (10 mM) was also tested either alone or in combination with above metal ions. The hydrolysis product, *PP_i (Huang & Yarus, 1997a), was separated from reactant *pppRNA by PEI TLC developed in 0.5 M potassium phosphate (pH 6.3) containing 20% methanol. ^{32}P was visualized and quantitated by a phosphorimager (BioRad GS525).

Kinetics of Decapping and Pyrophosphatase Activities of Isolate 6 RNA. Kinetics of decapping and pyrophosphatase activities of isolate 6 RNA were carried out at 37 °C and pH 5.5 (20 mM MES), 7.0 (20 mM HEPES), and 8.5 (20 mM Tris), respectively. Under various conditions (different Ca^{2+} concentrations, pH, presence of inhibiting metal ions), isolate 6 *pppRNA (0.1 μM) and G(5′)pppRNA (5 nM) were incubated for 5−120 and 20−1300 min, respectively. Three-microliter aliquots were taken out from reaction mixtures at different time intervals and quenched immediately by adding 3 μL of gel loading buffer containing 7 M urea, 10 mg/mL of xylene cyanol, and 40 mM EDTA. The samples were kept on ice until analysis by 18% denaturing gel (for pyrophosphatase, xylene cyanol = 0.5 cm) or by 8% denaturing gel (for decapping, xylene cyanol = 46 cm). Products (*PP_i and pRNA) and unreacted reactants [*pppRNA and G(5′)-pppRNA] were scanned by a phosphorimager and quantitated using peak integration from the Profile Analysis program (BioRad). Rate constants were derived from nonlinear fitting of experimental data with SigmaPlot (Jandel).

*Estimation of Decapping and Pyrophosphate-Releasing Rate of Random G(5′) *pppRNA and *pppRNA.* 5′[γ-^{32}P]-Labeled random 104mer G(5′)*pppRNA and *pppRNA were incubated in 20 mM MES and 2 mM $CaCl_2$, pH 5.5 for 110 h at 37 °C. As a control for $^{32}PP_i$ hydrolysis to $^{32}P_i$, $^{32}PP_i$ was also incubated under the same conditions. The reaction mixtures were chromatographed along with standards $^{32}P_i$, *pG, p*pG, and pp*pG (for decapping) and with standards $^{32}P_i$ and $^{32}PP_i$ (for pyrophosphate-releasing) on cellulose PEI TLC plates with 20% methanol and 80% 0.5 M potassium phosphate, pH 6.3. ^{32}P was visualized by phosphorimaging. Quantitation was as described above.

RESULTS

*Decapping Product of Isolate 6 G(5′) *pppRNA.* Self-capping isolate 6 pppRNA (Figure 1A) reacts with GDP to yield 5′ capped G(5′)pppRNA. The pppRNA can also release the 5′ pyrophosphate to generate pRNA in the presence or absence of GDP (Huang & Yarus, 1997a). Once capped, G(5′)pppRNA catalyzes release of its cap (see Figure 2 below).

To determine the hydrolysis product of the G(5′)pppRNA, we prepared 5′-[γ-^{32}P]-labeled isolate 6 G(5′)*pppRNA by reacting unlabeled isolate 6 pppRNA with [α-^{32}P]GTP in the presence of GTP:RNA guanylyltransferase and incubated the resulting G(5′)*pppRNA (after gel purification) in buffer containing Ca^{2+}. TLC analysis shows that the released ^{32}P-containing product is exclusively [α-^{32}P]GDP (p*pG) (Figure 1B). Therefore, as for the pyrophosphatase activity of the pppRNA, decapping of G(5′)pppRNA hydrolyzes the 5′ triphosphate linkage between the 5′ α- and β-phosphates and releases GDP:

$$H_2O\ (\text{nucleophile}) + G(5')\text{pppRNA (isolate 6)} \rightarrow \text{pRNA} + \text{GDP} \quad (4)$$

Divalent Metal Ion Requirement for Decapping. To determine the divalent metal ion requirement for the decapping activity, internally ^{32}P-labeled isolate 6 G(5′)pppRNA was incubated in solutions containing one or two different metal ions. The decapped pRNA was then separated from unreacted G(5′)pppRNA by 8% denaturing gel electrophoresis (Figure 2). While the RNA is active with a mixture of Mg^{2+} and Ca^{2+} (lane 3), which were present in the selection buffer (Huang & Yarus, 1997a), the G(5′)pppRNA is more

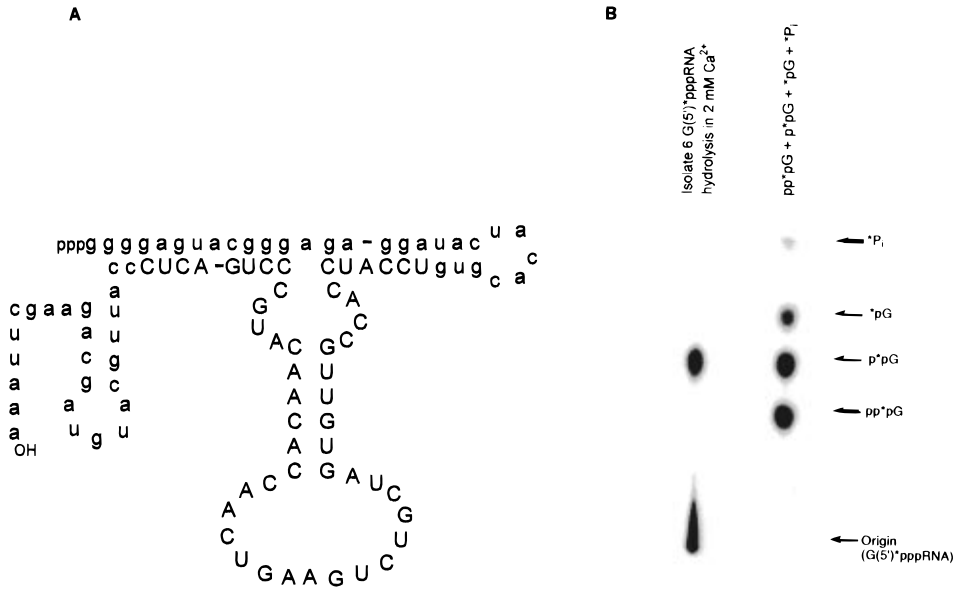

FIGURE 1: (A) Predicted secondary structure of isolate 6 RNA. The pictured secondary structure is a computed minimal free energy structure that is supported by lead cutting and nuclease S1 digestion. Capitalized nucleotides were initially randomized. (B) Decapping product of isolate 6 G(5′)*pppRNA. 5′[γ-^{32}P]-Labeled G(5′)*pppRNA was incubated for 4 h at 37 °C in 2 mM Ca^{2+} and 20 mM MES, pH 5.5. Released ^{32}P-containing product (p*pG) was separated from unreacted G(5′)*pppRNA by cellulose PEI TLC developed in 20% MeOH and 80% 0.5 M potassium phosphate, pH 6.3, and visualized by phosphorimaging.

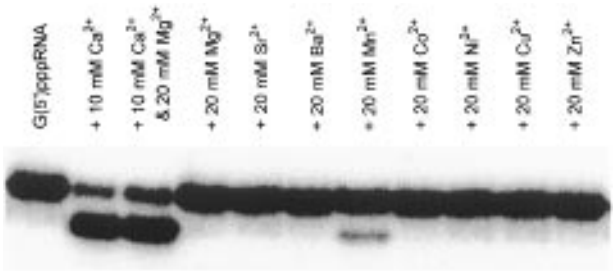

FIGURE 2: Metal ion requirement of 5′ decapping activity of isolate 6 G(5′)pppRNA. Internally ^{32}P-labeled G(5′)pppRNA was incubated for 3 h at 37 °C in 20 mM MES, pH 5.5, and metal ions as indicated. Decapped product (pRNA) was separated from unreacted G(5′)pppRNA by 8% denaturing PAGE (xylene cyanol = 46 cm) was visualized by phosphorimaging.

active with Ca^{2+} only (lane 2). Mg^{2+} alone does not activate the G(5′)pppRNA (lane 4). Mn^{2+}, also present during the selection (Huang & Yarus, 1997a), activates the RNA as well, although decapping activity is much lower (10−20%) with Mn^{2+} than with Ca^{2+}. Other divalent metal ions, Sr^{2+}, Ba^{2+}, Co^{2+}, Ni^{2+}, Cu^{2+}, and Zn^{2+}, at 20 mM each, do not support the decapping activity of isolate 6 G(5′)pppRNA.

Divalent Requirement for Pyrophosphatase. To determine the divalent metal ion requirement for pyrophosphatase activity, 5′ [γ-^{32}P]-labeled isolate 6 *pppRNA (104mer) was incubated with one divalent or trivalent metal ion in the presence or absence of spermidine. The released *PP_i (Huang & Yarus, 1997a) and *P_i were easily separated from reacted *pppRNA on TLC (Figure 3). While the *pppRNA hydrolyzed to near completion (85%) in 30 min in the presence of Ca^{2+}, no activity of the *pppRNA was detectable in the presence of other metal ions from the IIA group (Mg^{2+}, Sr^{2+}, and Ba^{2+}) (Figure 3A). However, Mn^{2+} can also activate the *pppRNA somewhat, producing 12% *PP_i in 30 min. Other metal ions at 10 mM, Co^{2+}, Ni^{2+}, Cu^{2+}, Zn^{2+}, Cd^{2+}, La^{3+}, Ce^{3+}, Sm^{3+}, and Dy^{3+}, are incapable of supporting pyrophosphatase activity of isolate 6 *pppRNA. In the presence of Cu^{2+}, the *pppRNA changes hydrolysis pattern, i.e., from cleavage between the 5′ α- and β-phosphates (producing *PP_i) in the presence of Ca^{2+} to cleavage between the 5′ β- and γ-phosphates (producing *P_i). In 30 min, the *pppRNA releases 15% *P_i in 10 mM Cu^{2+}. The *pppRNA is partially digested by Pb^{2+}, but it releases both *P_i (60%) and *PP_i (6%). However, hydrolysis in Cu^{2+} or Pb^{2+} is not RNA catalysis, since hydrolysis of random 104mer *pppRNA under the same conditions gives the same results in terms of both hydrolysis patterns and yields (data not shown). Adding 10 mM spermidine to solutions containing the above divalent or trivalent metal ions has no detectable effect on either hydrolysis pattern or yields (Figure 3B).

*Kinetics of Pyrophosphatase Activity of Isolate 6 *pppRNA.* Pyrophosphate release rates by *pppRNA were examined at the selection pH 5.5 (Huang & Yarus, 1997a) and at pH 7.0 and 8.5. Figure 4A shows one example of pyrophosphate release over 2 h in 1 mM Ca^{2+} and 20 mM MES, pH 5.5. The effect of Ca^{2+} concentration on the reaction is demonstrated in Figure 4B. The reaction does not go to completion, with 15% of the *pppRNA appearing unreactive (kinetics shown were performed directly with gel-purified RNA, but renaturation/refolding of the RNA did not affect kinetic behavior; data not shown). After inactive *pppRNA is subtracted, the reaction is first order in *pppRNA over more than 3 half-lives. As [Ca^{2+}] increases, the reaction speeds up, but the reaction approaches a constant rate at high [Ca^{2+}] (20 mM). Such a pyrophosphate release rate−[Ca^{2+}] relationship suggests saturation of an apparent Ca^{2+}-binding site. Treating Ca^{2+} as an equilibrating ligand and isolate 6 pppRNA as a Ca^{2+}-requiring enzyme, the apparent pyrophosphate release rate constant can be expressed as a function of [Ca^{2+}]:

$$k_{ob} = k_{cat}[Ca^{2+}]/(K_M + [Ca^{2+}]) \quad (5)$$

Double reciprocal Lineweaver−Burk plots with Ca^{2+} only, Ca^{2+} plus 4 mM Mg^{2+}, and Ca^{2+} plus 4 mM Sr^{2+} at pH 5.5

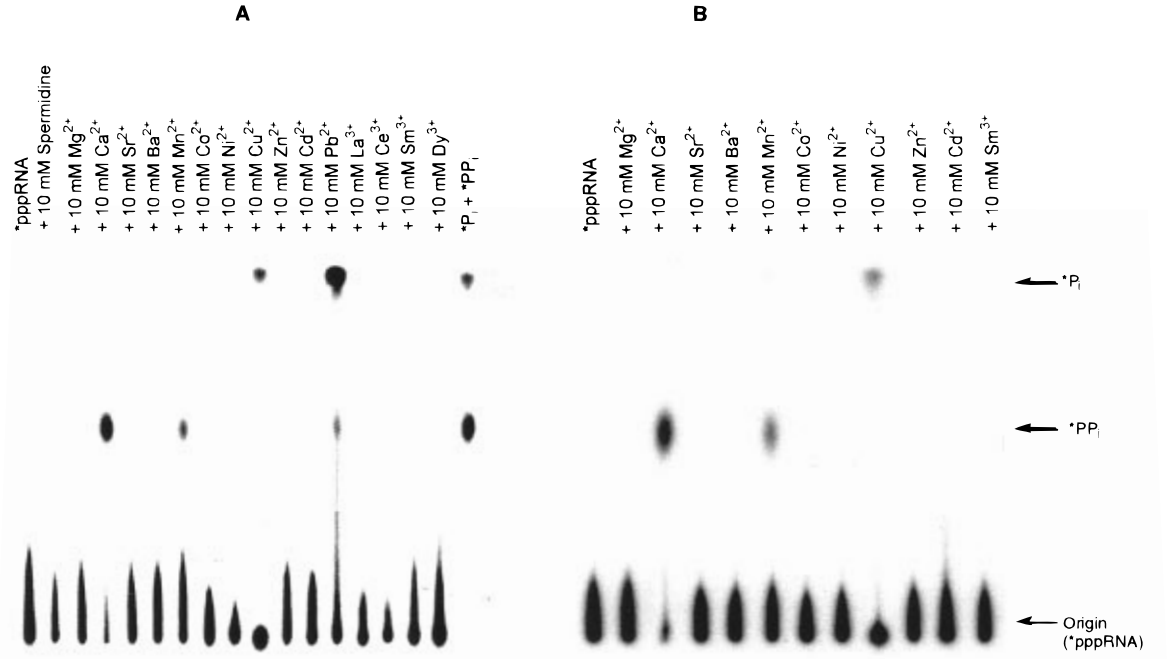

FIGURE 3: Divalent metal ion requirement of 5′ pyrophosphatase activity of isolate 6 pppRNA. (A) 5′[γ-^{32}P]-Labeled isolate 6 *pppRNA was incubated for 30 min at 37 °C in 20 mM MES, pH 5.5, and metal ions as indicated. (B) Same conditions as in A except for addition of 10 mM spermidine. Released *PPi was separated from unreacted *pppRNA by 18% denaturing PAGE (xylene cyanol = 0.5 cm) and visualized by phosphorimaging.

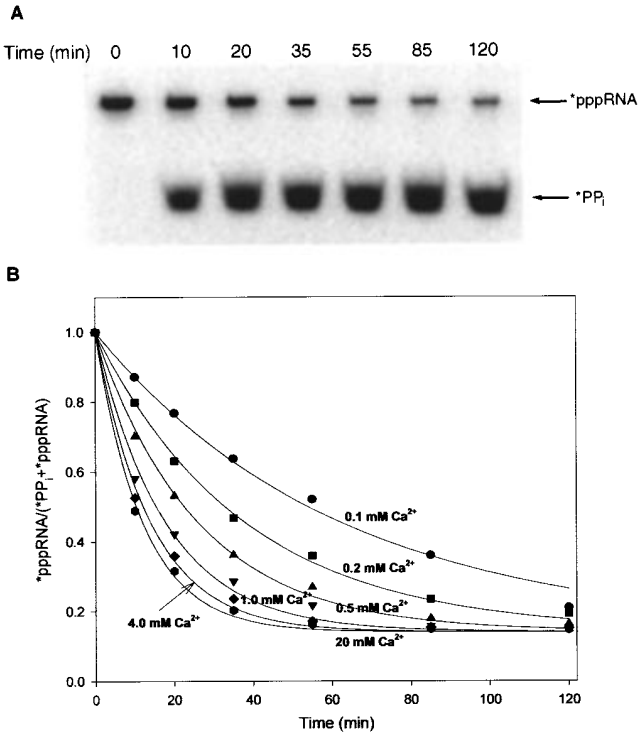

FIGURE 4: Pyrophosphosphate released by isolate 6 pppRNA over time. (A) 5′[γ-^{32}P]-Labeled *pppRNA was incubated for varying time intervals in 20 mM MES, pH 5.5, and 1.0 mM Ca^{2+} at 37 °C and then analyzed by 18% PAGE. (B) Effect of Ca^{2+} on *PP_i release of *pppRNA over time. Measured concentrations of *pppRNA are represented by dots, while the line is the fitted first-order reaction after subtracting 14% unreactive *pppRNA.

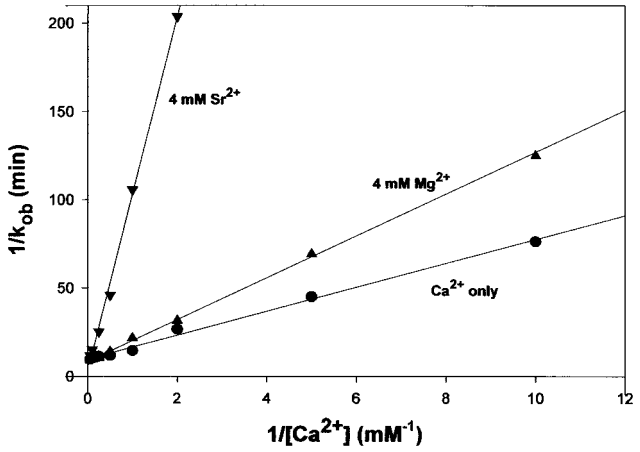

FIGURE 5: Lineweaver−Burk plots of pyrophosphatase activity of isolate 6 pppRNA at pH 5.5 and 37 °C in the presence or absence of Mg^{2+} or Sr^{2+}.

Table 1: Kinetic Parameters of Pyrophosphatase Activity of Isolate 6 pppRNA at 37 °C[a]

parameter	pH 5.5	pH 7.0	pH 8.5
k_{cat} (min^{-1})	0.10 ± 0.01	0.032 ± 0.003	0.011 ± 0.001
K_M (Ca^{2+}) (mM)	0.7 ± 0.1	0.06 ± 0.01	0.04 ± 0.01
k_{cat}/K_M (Ca^{2+}) (M^{-1}·min^{-1})	150 ± 20	500 ± 100	360 ± 80
K_i (Mg^{2+}) (mM)	5.6 ± 0.9	ND	ND
K_i (Sr^{2+}) (mM)	0.29 ± 0.04	ND	ND

[a] Buffers used: 20 mM MES (pH 5.5), HEPES (pH 7.0), and Tris (8.5). ND = not determined.

are shown in Figure 5; the model clearly fits observed behavior well. Mg^{2+} and Sr^{2+} change the apparent Michaelis−Menten constant $K_M{}^{A}{}_{pp}$ but do not change the maximum rate constant k_{cat} which indicates that Mg^{2+} and Sr^{2+} are competitive inhibitors at the Ca^{2+} site(s), with Sr^{2+} being a much stronger inhibitor than Mg^{2+}. Inhibition constants, K_i-(Mg^{2+}) and K_i(Sr^{2+}), were calculated from their corresponding $K_M{}^{App}$, $K_i = [I]/(K_M{}^{App}/K_M - 1)$. Kinetic parameters for the pyrophosphatase of isolate 6 pppRNA are listed in Table 1.

Pyrophosphatase as a Function of pH. The pppRNA still behaves as a Ca^{2+}-dependent enzyme even at pH 8.5, three units higher than the selection pH 5.5 (Huang & Yarus,

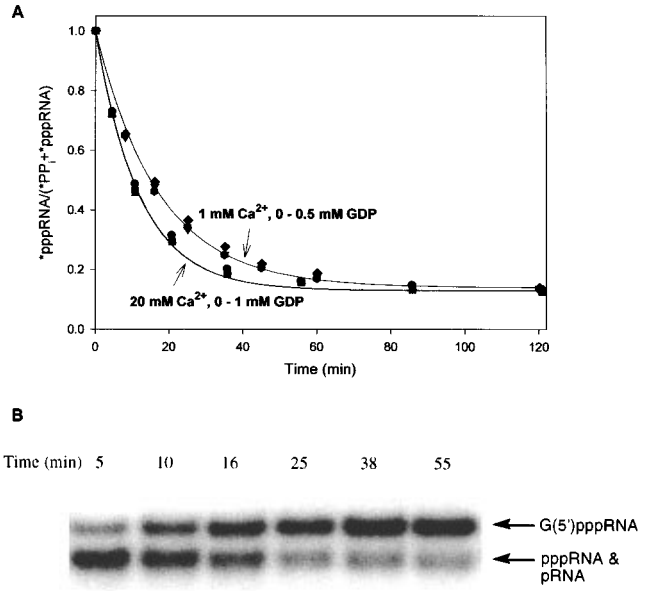

FIGURE 6: (A) Effect of GDP on pyrophosphate release rate of *pppRNA at 1 and 20 mM Ca^{2+}. The pyrophosphate release is unchanged in the presence of 0, 0.1, 0.5, and 1.0 mM GDP. (B) Capping reaction of internally ^{32}P-labeled pppRNA in 1 mM GDP, 20 mM MES, and 20 mM Ca^{2+} at pH 5.5. After GDP capping, the reaction mixture was analyzed on a 8% denaturing gel and visualized by phosphorimaging.

1997a). As at pH 5.5, the pyrophosphatase activity increases with [Ca^{2+}] and approaches a V_{max} at a given pH. However, saturating [Ca^{2+}] is much lower at pH > 7 than at pH 5.5. Kinetic parameters k_{cat} and K_M are well defined in the Lineweaver−Burk plots (data not shown) and are listed in Table 1. Increasing pH not only decreases the maximum rate constant k_{cat}, but also remarkably reduces the Michaelis−Menten constant K_M. The catalytic efficiency, k_{cat}/K_M, also changes with pH (Table 1), but influence of pH is relatively small (3-fold change within pH 5.5−8.5) due to a parallel effect of pH on k_{cat} and K_M. At pH 7.0 or higher, a strong pppRNA−Ca^{2+} Michaelis complex with an apparent dissociation constant of 40−60 μM is suggested by the K_M (see Discussion).

Kinetics have not been examined at pH <5.5 or >8.5, but the *pppRNA releases 14% and 24% of its 5′ pyrophosphate in 30 min at 37 °C in 2 mM Ca^{2+} and 20 mM acetate buffer, pH 4.5 and 5.0, respectively. On the other hand, ~70% *PP_i is released in 2 mM Ca^{2+} and 20 mM MES buffer, pH 5.5. The *pppRNA hydrolyzes 16% *PP_i in 30 min at 37 °C in 2 mM Ca^{2+} and 20 mM Tris buffer, pH 9.0, compared to 18% *PP_i release under the same conditions except at pH 8.5. These results indicate that the 5′ pyrophosphatase activity of isolate 6 pppRNA is highest at selection pH 5.5.

A Constant Total Rate. Surprisingly, overall pyrophosphate release from the *pppRNA is not affected by GDP (Figure 6A). At 1 or 20 mM Ca^{2+} in 20 mM MES, pH 5.5, release of *PP_i by *pppRNA follows the same time course with GDP concentrations of 0, 0.1, 0.5, to 1.0 mM. While the above results indicate a constant overall pyrophosphate release rate at a a given Ca^{2+} concentration, regardless of GDP's presence, GDP-capping yield of the pppRNA reaches 70% in 20 mM Ca^{2+} and 1 mM GDP (Figure 6B). Because overall pyrophosphate release is the sum of GDP-capping (releasing PP_i, reaction 1) rate and water-dependent pyrophosphate-releasing (reaction 2) rate and capping reaches 70%, it follows that GDP suppresses the pyrophosphatase activity of the pppRNA, while the combination of the two activities remains unchanged at a given Ca^{2+} concentration.

Kinetics of Decapping Activity by G(5′)pppRNA. Kinetics of the decapping activity of isolate 6 G(5′)pppRNA were conducted at selection pH 5.5 (Huang & Yarus, 1997a) and at pH 7.0 and 8.5. Figure 7A shows one example of GDP release during 21 h in 20 mM Ca^{2+}, pH 5.5. The effect of Ca^{2+} concentration on the decapping rate of isolate 6 G(5′)-pppRNA is demonstrated in Figure 7C. Unlike pyrophosphate release by isolate 6 pppRNA, which is a first-order reaction for the 85% reactive fraction (see above), the decapping reaction can go to completion (see Figure 10B below), but it does not fit a first-order rate in G(5′)pppRNA (Figure 7B). Instead, a rate equation with the order 1.5 in G(5′)pppRNA fits the experimental data over more than 3 half-lives (although the experiments were conducted directly with gel-purified RNA, renaturation/refolding did not change kinetics; data not shown). However, increasing G(5′)-pppRNA concentration from 5 to 100 nM (in 20 mM Ca^{2+}) does not change the fraction decapped vs a time curve (data not shown). For the nth order reaction in reactant A, $d[A]/dt = -k[A]^n$. When expressed in fraction f ($f = [A]/[A]_0$), then $df/dt = -k[A]_0^{(n-1)}f^n$. Integration of the equation yields the fraction−time relationship of reactant A: $f = 1 - e^{-kt}$ if $n = 1$ and $f = \{1 + (n - 1)kt[A]_0^{(n-1)}\}^{(n-1)}$ if $n \neq 1$. Therefore, only the fraction−time curve of a first order-reaction is independent of initial concentration of the reactant.

Treatment of the Decapping Rate Constants. Since the concentration−time relationship of isolate 6 decapping does not change when increasing the reactant initial concentration from 5 to 100 nM, we believe that the decapping of G(5′)-pppRNA is a first-order reaction, as is the pyrophosphatase activity of the pppRNA. To explain an apparent reaction order of 1.5, there may exist active and inactive conformations. Slow conversion from inactive to active conformations of the RNA or other complications that slow reaction slightly may result in an apparent overall 1.5th order of reaction (Figure 7B). Renaturation of the G(5′)pppRNA does not change its kinetics, indicating that this unusual behavior is probably not caused by a nonequilibrated inactive conformation. One other possibility, product inhibition, can be ruled out as the explanation of the observed reaction order: G(5′)-pppRNA concentration is too low (5 nM). Even at 1 μM, exogenously added GDP has no observable effect on decapping (see Figure 9 below).

All kinetic data were fitted to an observed 1.5th order equation ($df/dt = -kf^{1.5}$) to derive the rate constant k, which is equivalent to an initial reaction rate (when $f = 1$). Since we have other evidence that the true reaction is first order, the initial reaction rate should be equal to its first-order rate constant ($df/dt = -kf = k$, when $f = 1$). Therefore, rate constants derived from experimental fitting are treated as first order, with units of min^{-1}. Rate constants derived directly from fitting the reaction course as first order are smaller by ≤30% (Figure 7B), and the experimental data lie reproducibly off the fitted curve.

Decapping and Ca^{2+}. Decapping rate accelerates as [Ca^{2+}] increases, and the reaction approaches a constant rate at high [Ca^{2+}] (100 mM), which suggests the formation of a Ca^{2+}−G(5′)pppRNA complex. Figure 8 shows Lineweaver−Burk plots with Ca^{2+} only, Ca^{2+} plus 20 mM Mg^{2+},

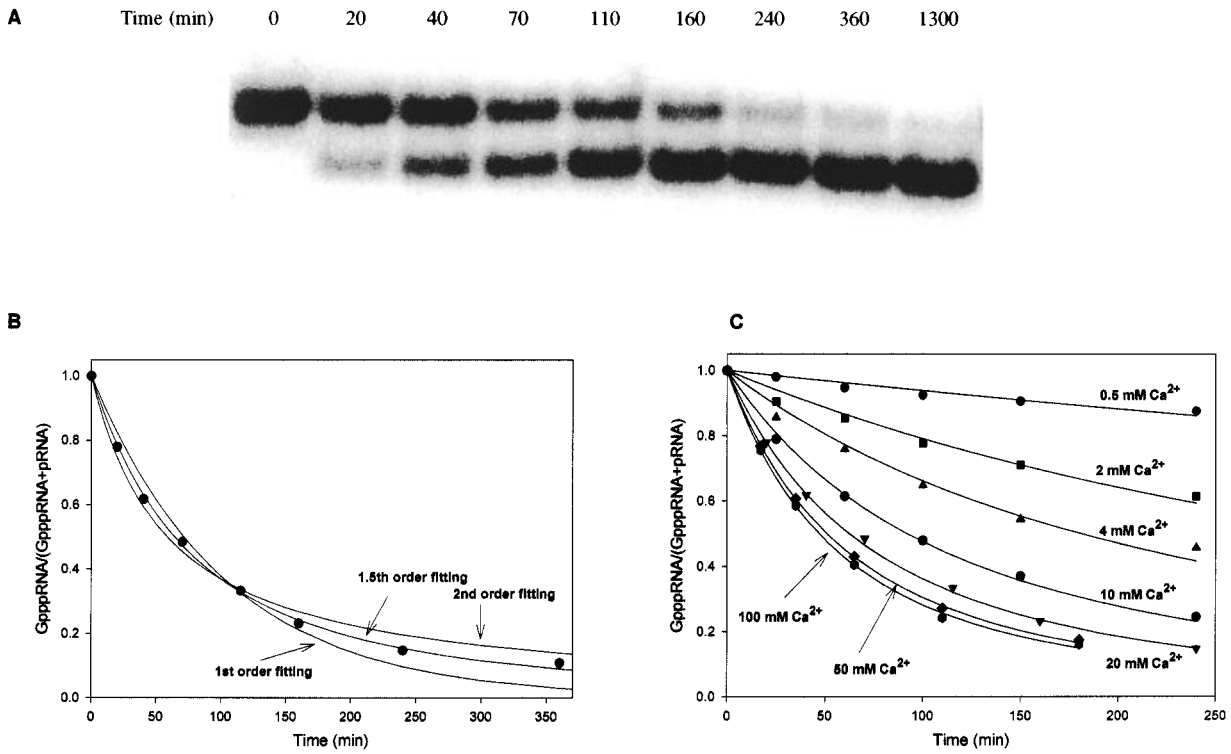

FIGURE 7: Decapping time course of isolate 6 G(5′)pppRNA. (A) Internally ^{32}P-labeled G(5′)pppRNA was incubated for varying time intervals in 20 mM Ca^{2+} and 20 mM MES, pH 5.5, at 37 °C and then analyzed by 8% PAGE. (B) Fitting of concentration (expressed in fraction)−time curve to first-, 1.5th-, and second-order equations. The data are best fitted by the 1.5th-order equation. (C) Effect of Ca^{2+} on decapping over time. Measured concentration (in fraction) of G(5′)pppRNA are represented by dots, while the lines are fitted curves (1.5th order, see text for rationale).

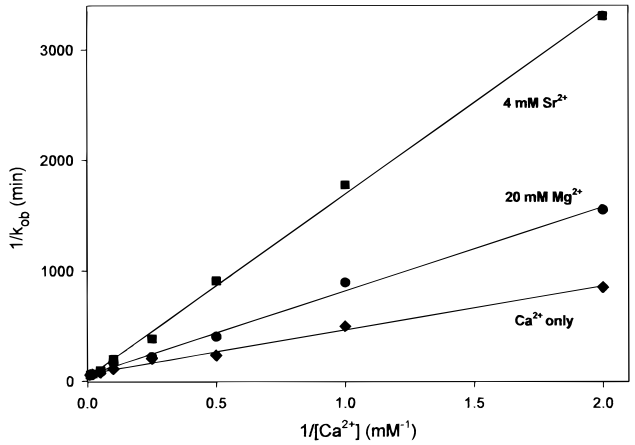

FIGURE 8: Lineweaver−Burk plots of decapping activity of isolate 6 G(5′)pppRNA at pH 5.5 and 37 °C in the presence or absence of Mg^{2+} or Sr^{2+}.

and Ca^{2+} plus 4 mM Sr^{2+} at pH 5.5. Like the pppRNA, when Ca^{2+} varies the G(5′)pppRNA behaves as an enzyme saturating with the divalent, with a well-defined maximum rate constant k_{cat} and a Michaelis−Menten constant K_M for the formation of a G(5′)pppRNA−Ca^{2+} complex. Mg^{2+} and Sr^{2+} act as competitive inhibitors, indicated by their ability to change the apparent Michaelis−Menten constant K_M^{App} but not the maximum rate constant k_{cat}. Kinetic parameters for isolate 6 G(5′)pppRNA are listed in Table 2.

A Constant Total Rate. GDP decreases the apparent decapping rate of isolate 6 G(5′)pppRNA (Figure 9). Decapping rate constants are 2.6, 1.8, 0.44, and 0.17 × 10^{-3} min^{-1} at 2 mM Ca^{2+} in 0, 0.01, 0.1, and 1 mM GDP, respectively, and 13, 8.5, 2.0, and 0.64 × 10^{-3} min^{-1} at 20 mM Ca^{2+} in 0, 0.01, 0.1, and 1 mM GDP, respectively. These

Table 2: Kinetic Parameters of Decapping Activity of Isolate 6 G(5′)pppRNA at 37 °C[a]

parameter	pH 5.5	pH 7.0	pH 8.5
k_{cat} (min^{-1})	0.018 ± 0.002	0.012 ± 0.001	0.0023 ± 0.0002
K_M (Ca^{2+}) (mM)	6 ± 2	0.23 ± 0.05	0.1 ± 0.02
k_{cat}/K_M (Ca^{2+}) ($M^{-1}min^{-1}$)	3 ± 1	50 ± 15	23 ± 5
K_i (Mg^{2+}) (mM)	15 ± 4	ND	ND
K_i (Sr^{2+}) (mM)	1 ± 0.2	ND	ND

[a] The rate constants are derived from 1.5th order fitting of experimental data but considered as first-order rate constants (see text for rationale). Buffers used: 20 mM MES (pH 5.5), HEPES (pH 7.0), and Tris (8.5). ND = not determined.

rates correspond to 30−35%, 80−85%, and 90−95% decreases in decapping rate in the presence of 0.01, 0.1, and 1 mM GDP. One micromolar GDP has no observable effect. Reduction in decapping rate by GDP is not due to a reverse reaction with added GDP because decapped pRNA cannot react with GDP to form the capped G(5′)pppRNA (Huang & Yarus, 1997a). Instead, GDP exchange with G(5′)-pppRNA slows the decapping reaction (see Discussion).

Decapping of isolate 6 G(5′)pppRNA to pRNA is also decreased by guanosine 5′-tetraphosphate (ppppG) (Figure 10). However, a new capped G(5′)ppppRNA is formed in addition to decapped pRNA. Since the pRNA is unreactive (Huang & Yarus, 1997a), the capped G(5′)ppppRNA is produced by a cap exchange reaction of the G(5′)pppRNA:

$$\text{ppppG (nucleophile)} + \text{G(5′)pp}\mathbf{p}\text{RNA (isolate 6)} \rightarrow \text{G(5′)ppppp}\mathbf{p}\text{RNA} + \text{GDP} \quad (6)$$

Using the PeakFit program (Jandel), concentrations of G(5′)-pppRNA, G(5′)ppppRNA, and pRNA were obtained from

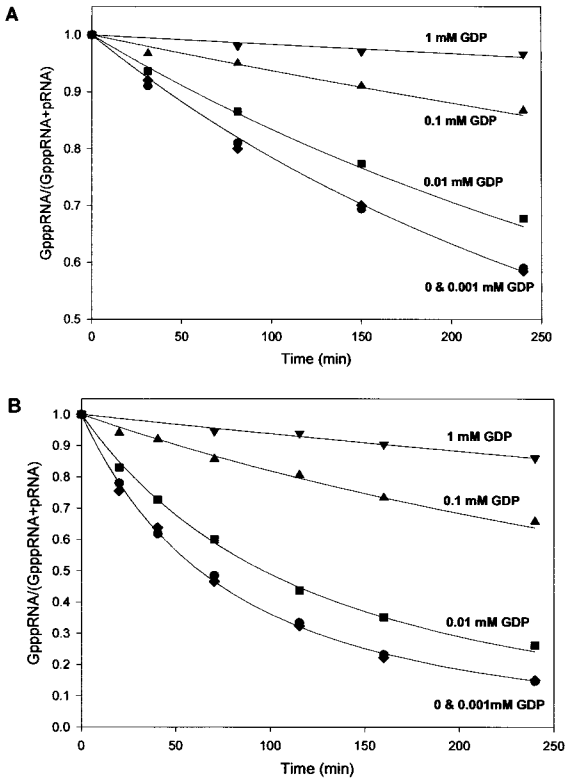

FIGURE 9: Effect of GDP on decapping of isolate 6 G(5′)pppRNA. At 2 and 20 mM Ca^{2+}, GDP decreases the decapping rate of the capped RNA, while 1 μM GDP has no apparent effect.

peak integration (Figure 10B). The disappearance of G(5′)-pppRNA follows the same time course [e.g., apparent 1.5th order in G(5′)pppRNA] as without ppppG in Figure 7. Thus, ppppG does not affect the disappearance rate of the G(5′)-pppRNA. However, the decapping (forming pRNA) and exchange [producing G(5′)ppppRNA] reactions compete, and exchange is much faster than the decapping. According to the scheme in Figure 10B, the rates for the formation of G(5′)ppppRNA and pRNA can be expressed as:

$$\mathrm{d[G(5')ppppRNA]/d}t = k_1[\mathrm{G(5')pppRNA}]^{1.5} - k_2[\mathrm{G(5')ppppRNA}]^{1.5} \quad (7)$$

$$\mathrm{d[pRNA]/d}t = k_2[\mathrm{G(5')ppppRNA}]^{1.5} + k_3[\mathrm{G(5')pppRNA}]^{1.5} \quad (8)$$

For curve-fitting purposes, we assume 1.5th order reactions for the starting G(5′)pppRNA (see above) and the newly generated G(5′)ppppRNA, all expressed as fractions. However, the rate constants are considered as first-order constants with the unit of min^{-1} (see above).

To obtain the rate constants k_1, k_2, and k_3, the derivatives d[G(5′)ppppRNA]/dt and d[pRNA]/dt were calculated from the two curves marked G(5′)ppppRNA and pRNA in Figure 10B. The experimental data were then fitted nonlinearly according to eqs 7 and 8 using SigmaPlot (Jandel). The values (in 1 mM ppppG and 20 mM Ca^{2+} at pH 5.5) thus

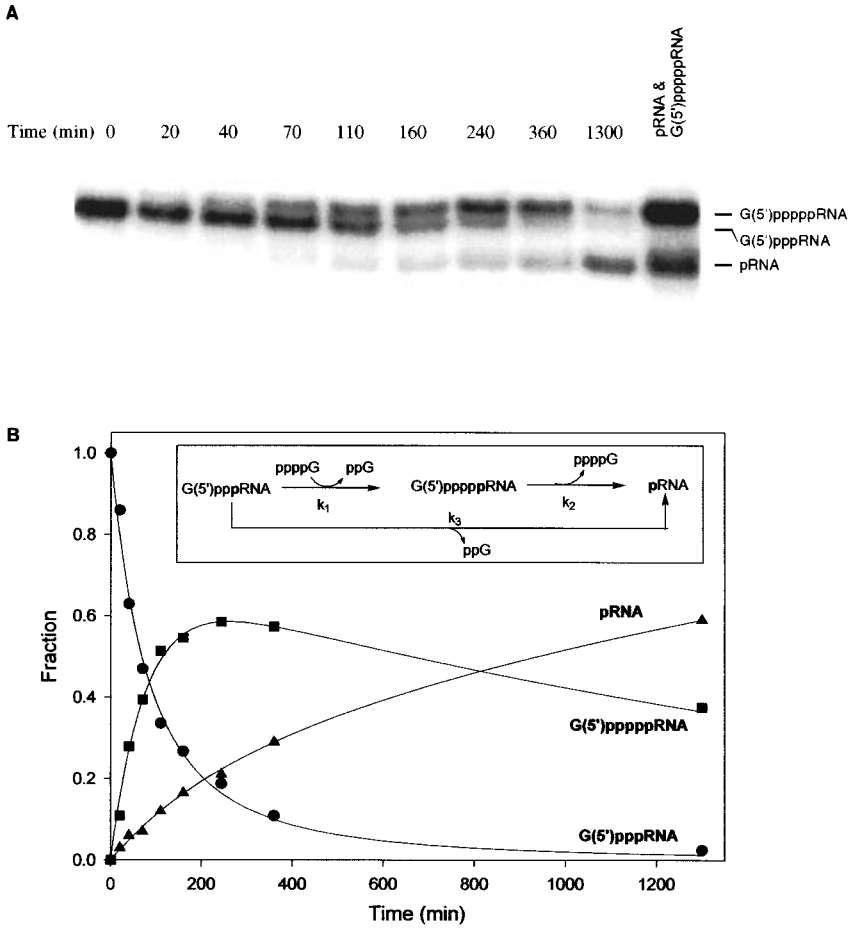

FIGURE 10: Decapping and exchange reaction of isolate 6 G(5′)pppRNA with guanosine 5′-tetraphosphate (ppppG, 1 mM) in 20 mM Ca^{2+} and 20 mM MES, pH 5.5, at 37 °C. Measured concentrations (in fractions) of G(5′)pppRNA, G(5′)ppppRNA, and pRNA are represented by dots, while the lines are the fitting curves (see text for details). Standard G(5′)ppppRNA in the last lane was prepared by reacting isolate 6 pppRNA with 1 mM ppppG in 2 mM Ca^{2+} and 20 mM MES (pH 5.5) for 1 h at 37 °C (Huang & Yarus, 1997b).

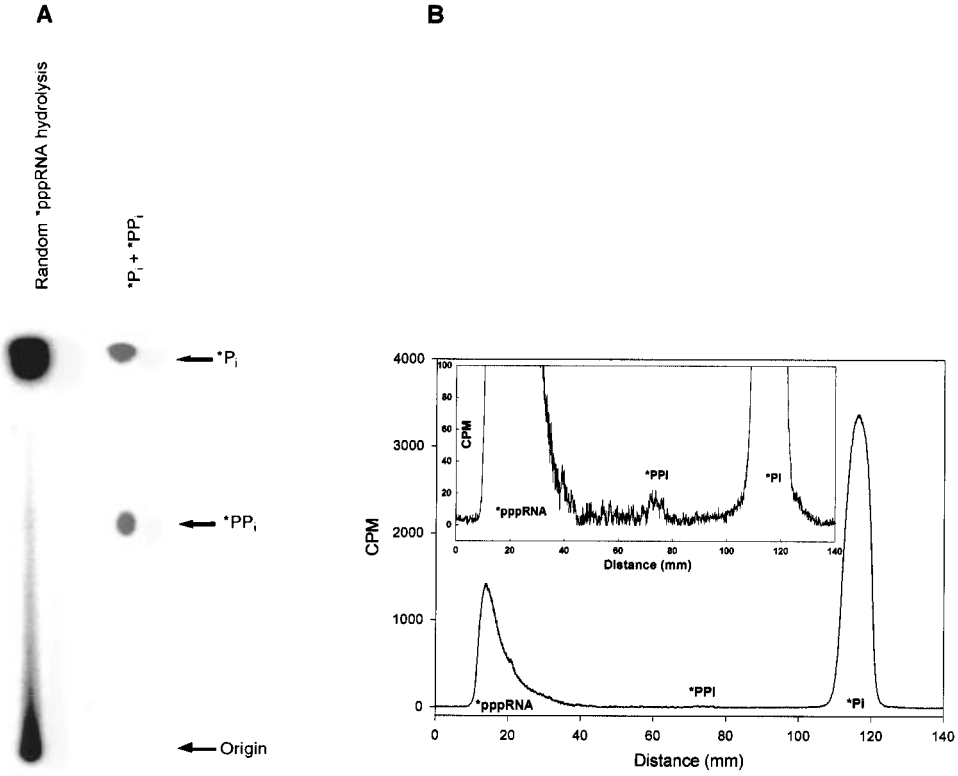

FIGURE 11: Estimation of 5′ pyrophosphate release rate of random 104mer pppRNA in 2 mM Ca^{2+} and 20 mM MES, pH 5.5 at 37 °C. (A) Hydrolysis product (after 110 h) analysis by TLC (PEI), developed in 20% methanol and 80% 0.5 M potassium phosphate, pH 6.3. (B) Profile of ^{32}P-counts on the TLC plates, analyzed by Profile Analysis (BioRad) using a straight line as base-line correction. Quantitation of *P_i and *PP_i was obtained through peak integration.

derived are 0.011 ± 0.001, 0.0018 ± 0.0005, and 0.0014 ± 0.0005 min^{-1} for k_1, k_2, and k_3, respectively. Therefore, the exchange reaction (represented by k_1) of G(5′)pppRNA with ppppG (1 mM) is about eight times faster than the decapping reaction (represented by k_3), which is 10−15% of the decapping rate in the absence of GDP or ppppG. On the other hand, the two decapping reactions for G(5′)pppppRNA and G(5′)pppRNA in the presence of 1 mM ppppG proceed with similar rates (comparing k_2 and k_3).

At higher pH, decapping of the G(5′)pppRNA is slower at millimolar [Ca^{2+}]. Although k_{cat} is lower at pH ≥ 7 than at pH 5.5, K_M decreases faster than k_{cat}. As a result, the catalytic efficiency, k_{cat}/K_M, increases with pH (Table 2). As in the case of the pyrophosphatase activity, a strong G(5′)-pppRNA−Ca^{2+} complex with an apparent dissociation constant of 100−200 μM is suggested by K_M at pH 7.0 or higher.

Decapping yields at pH <5.5 or >8.5 have been determined at 120 min and 37 °C. The G(5′)pppRNA releases 2.5% and 3.9% of the 5′ cap GDP in 2 mM Ca^{2+} and 20 mM acetate buffer, pH 4.5 and 5.0, respectively. At pH 9.0 in 2 mM Ca^{2+} and 20 mM Tris buffer, 6.3% pRNA is produced from the G(5′)pppRNA, while 14.2% G(5′)-pppRNA decapping occurs at pH 8.5. In comparison with ∼20% GDP release in 2 mM Ca^{2+} and 20 mM MES buffer (pH 5.5), these results indicate that, as for the 5′ pyrophosphatase activity of the pppRNA, the 5′ decapping activity of isolate of 6 G(5′)pppRNA is highest at or near selection pH 5.5.

*Pyrophosphate Release by Random *pppRNA.* To compare the pyrophosphatase activity of isolate 6 pppRNA with background pyrophosphate hydrolysis of random pppRNA, 5′[γ-^{32}P]-labeled random *pppRNA (104mer) was incubated at 37 °C in 20 mM MES, 2 mM $CaCl_2$, pH 5.5. Figure 11A shows the hydrolysis result (by PEI TLC) of 104mer random *pppRNA after 110 h incubation. Figure 11B is the profile of ^{32}P-activity. The major product from the hydrolysis of random *pppRNA is orthophosphate (*P_i), and pyrophosphate (*PP_i) represents only a very small fraction of the product (Figure 11B). By integration of the profile (Figure 11B), *P_i and *PP_i represent 61.2% and 0.25% total ^{32}P-counts, respectively. We can calculate from these data that the 104mer random pppRNA hydrolyzes to P_i and PP_i with apparent first-order rate constants of 1×10^{-4} and 4×10^{-7} min^{-1}, respectively. By similar analysis of *PP_i hydrolysis under the above conditions, PP_i hydrolyzes to P_i with a calculated first-order rate constant of 6×10^{-7} min^{-1}. The hydrolysis rate constant of PP_i obtained here (at 37 °C) is consistent with a published value of 1×10^{-7} min^{-1} at 25 °C (Hubner & Milburn, 1980) after the temperature difference is taken into account. Considering the hydrolysis of PP_i to P_i, the hydrolysis of pppRNA to PP_i can be written (assuming first-order reactions):

$$\text{pppRNA} \xrightarrow{k_1} \text{pRNA} + \text{PP}_i \tag{9}$$

$$\text{PP}_i \xrightarrow{k_2} 2\text{P}_i \tag{10}$$

$$\text{pppRNA} \xrightarrow{k_3} \text{ppRNA} + \text{P}_i \tag{11}$$

$$[\text{PP}_i] = k_1[\text{pppRNA}]_0(\mathbf{e}^{-(k_1+k_3)t} - \mathbf{e}^{-k_2 t})/(k_2 - k_1 - k_3) \tag{12}$$

A k_1 value of 5×10^{-7} min^{-1} is obtained from eq 12, using $k_2 = 6 \times 10^{-7}$ min^{-1}, $k_3 = 1 \times 10^{-4}$ min^{-1}, $t = 110$

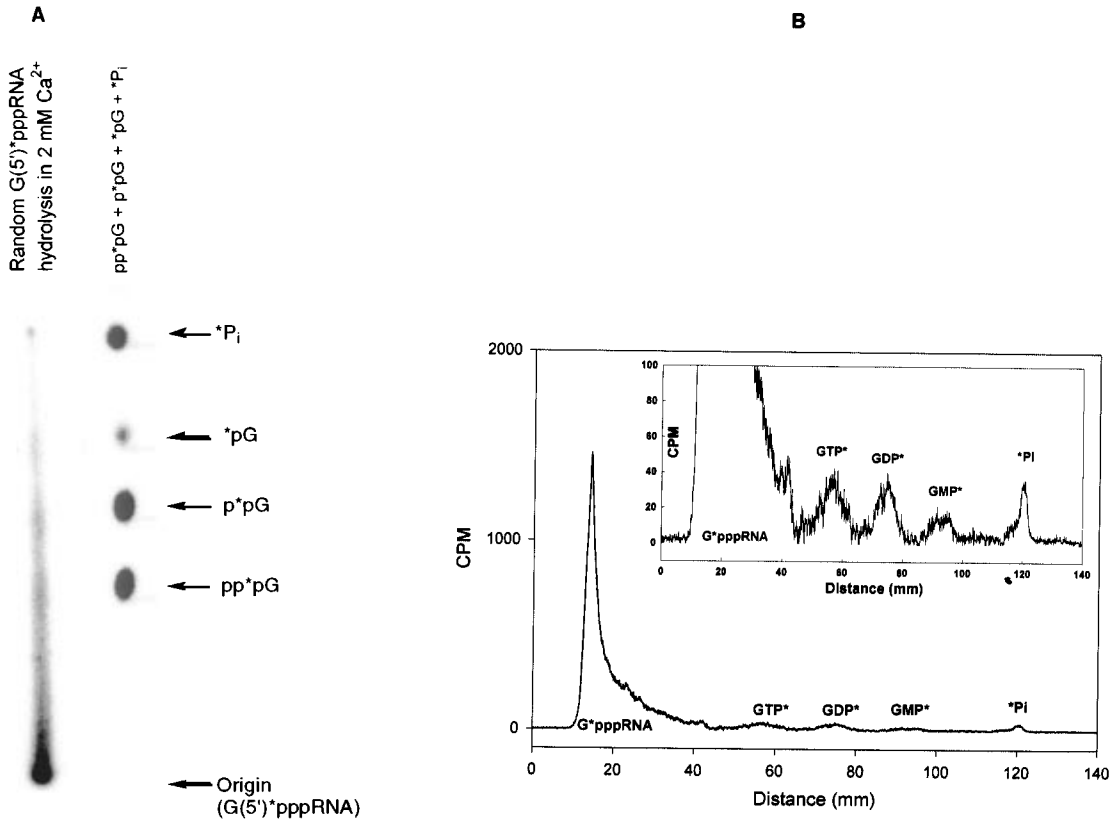

FIGURE 12: Estimation of 5′ pyrophosphate release rate of random 104mer pppRNA in 2 mM Ca^{2+} and 20 mM MES, pH 5.5 at 37 °C. (A) Hydrolysis product (after 110 h) analysis by TLC (PEI), developed in 20% methanol and 80% 0.5 M potassium phosphate at pH 6.3. (B) Profile of ^{32}P-counts on the TLC plate, analyzed by Profile Analysis (BioRad) using straight line base-line correction. Quantitation of $*P_i$ and $*PP_i$ was obtained through peak integrations.

h, $[PP_i] = 0.25\%$, and $[pppRNA]_0 = 100\%$ at 37 °C. Under the same conditions, isolate 6 pppRNA releases its 5′ pyrophosphate with a rate constant of 0.084 min^{-1}. Therefore, the 5′ pyrophosphatase activity of selected isolate 6 pppRNA is 170 000-fold accelerated with respect to 5′ pyrophosphate release from unselected random 104mer pppRNA in 2 mM Ca^{2+}, pH 5.5.

*Decapping of Random G(5′)*pppRNA.* To estimate the decapping activity of isolate 6 G(5′)pppRNA over background decapping of random G(5′)pppRNA, 5′[γ-^{32}P]-labeled random 104mer G(5′)*pppRNA (prepared by guanylyltransferase in the presence of [α-^{32}P]GTP and gel purified) was incubated at 37 °C in 20 mM MES, 2 mM $CaCl_2$, pH 5.5. Figure 12A shows hydrolysis products (by PEI TLC) from random G(5′)*pppRNA after 110 h incubation, and Figure 12B is the profile of ^{32}P-activity after a straight base-line correction. There are four ^{32}P-containing products in comparable amounts, 1.4% $*P_i$, 1.1% *pG (GMP*), 2.0% p*pG (GDP*), and 2.3% pp*pG (GTP*), which correspond to hydrolysis reactions with calculated first-order rate constants of (2.1, 1.7, 3.0, and 3.5) $\times$ 10^{-6} min^{-1}, respectively. Therefore, the hydrolysis of random capped G(5′)pppRNA appears to occur in a random cleavage pattern among the 5′triphosphates with rate constants of $2-3 \times 10^{-6}$ min^{-1} (total rate constant $\sim 1 \times 10^{-5}$ min^{-1}). On the other hand, under the same conditions, isolate 6 G(5′)pppRNA releases its 5′ GDP (specific cleavage between the 5′ α- and β-phosphates) with a rate constant of 0.0026 min^{-1}. That is, isolate 6 G(5′)pppRNA has a 5′ decapping activity $\sim$1000-fold above 5′ GDP release of unselected random 104mer G(5′)pppRNA in 2 mM Ca^{2+}, pH 5.5.

During the hydrolysis of random pppRNA and G(5′)-pppRNA, nonspecific RNA degradation is minimal (Figure 7A) for over more than 20 h of incubation. Therefore, the error in these rates due to degradation of RNA is negligible.

DISCUSSION

Isolate 6 RNA, selected *in vitro* (Huang & Yarus, 1997a), has three distinct catalytic activities centered at the 5′ α-phosphate: the general phosphoryl coupling (self-capping with phosphates is a specific case; Huang & Yarus, 1997a, 1997b), the pyrophosphatase, and the general decapping described above. Although there are three phosphates (α, β, and γ) at the 5′ end of the RNA, all three activities are highly specific for attack at the α-phosphate. During the reaction, a nucleophile (Nu = water or terminal phosphate containing molecules) is linked to the α-phosphate with a concurrent cleavage between the α- and β-phosphates:

$$Nu + Rpp{-}\mathbf{p}RNA \rightarrow Rpp + Nu\text{-}\mathbf{p}RNA \qquad (13)$$

Where Rpp can be pyrophosphate, GDP, or a ppppG molecule.

The number of capping reactants for this RNA is very large, ranging from small molecules such as PP_i to phosphorylated amino acids and sugars and to nucleotides and macromolecules like other RNAs (Huang & Yarus, 1997b). This corresponds to the initial selection for this catalyst, which was for any mode of release of the 5′ pyrophosphate from a pool of randomized RNA transcripts (Huang & Yarus, 1997a). This intrinsic lack of specificity allowed us to demonstrate that several interesting products, presumably

accessed via similar transition states, were within the capabilities of RNA catalysis acting on biological substrates. For example, the eukaryotic mRNA cap (Huang & Yarus, 1997a) and precise and covalent cofactor-RNAs (Huang & Yarus, 1997b) can be produced by similar reactions. We have now shown that such capped RNAs can be stabilized by control of the decapping reaction through simple mechanisms such as metal ion concentrations, inhibiting metal ions, pH, and "substrate" concentrations. Such additions to the versatility of RNA catalysis increasingly support the concept that a world of RNA-based chemical transformations existed before the emergence of modern cellular life (White, 1976; Gilbert, 1986; Joyce, 1989; Huang & Yarus, 1997a, 1997b).

All three activities have the same unique metal ion requirement for Ca^{2+} or Mn^{2+} (Mn^{2+} has 10−20% activity of Ca^{2+}). Other metal ions, including Mg^{2+}, Sr^{2+}, Ba^{2+}, Co^{2+}, Ni^{2+}, Cu^{2+}, Zn^{2+}, Cd^{2+}, La^{3+}, Ce^{3+}, Sm^{3+}, and Dy^{3+}, do not support the activities even in the presence of a polyamine. The three activities also exhibit similar broad active pH range (tested from pH 4.5 to 9.0) and are most active at or near selection pH 5.5 (Huang & Yarus, 1997a).

Hydrolysis of random pppRNA occurs predominantly between the 5′ β- and γ-phosphates in 2 mM Ca^{2+} and 20 mM MES, pH 5.5, releasing P_i (Figure 11). The release of PP_i is minor but detectable by the TLC method used. Hydrolysis of random pppRNA resembles that of ATP. ATP releases its 5′ γ-phosphate to produce ADP and P_i at acidic pH with or without Ca^{2+}; PP_i is not a detectable hydrolysis product (Hock & Huber, 1956; Liebecq & Jacquemotte-Louis, 1958). ATP hydrolysis in water at pH 4−6 and 37 °C is estimated to have a rate constant of 3×10^{-5} min^{-1} (Liebecq & Jacquemotte-Louis, 1958; Hulett, 1970). Ca^{2+} (20 mM) accelerates the hydrolysis about 2-fold at pH 5 (Tetas & Lowenstein, 1963). Therefore, ATP hydrolysis (from ATP → ADP + P_i) in 2 mM Ca^{2+} at pH 5.5 and 37 °C can be estimated to have a rate of $(3-6) \times 10^{-5}$ min^{-1}. Under the same conditions, random pppRNA hydrolyzes to ppRNA and P_i with a rate constant of 1×10^{-4} min^{-1}. Both random pppRNA and ATP hydrolyze their 5′ phosphates with the same specificity (cleavage between 5′ β- and γ-phosphates) and proceed with similar rates. Since hydrolysis of different NTPs is almost identical (Sigel & Hofstetter, 1983) and Ca^{2+} exerts little effect on hydrolysis of ATP (Tetas & Lowenstein, 1963), the hydrolysis of random pppRNA initiated with GTP (Huang & Yarus, 1997a) also resembles that of ATP. Thus, under the above hydrolysis conditions, the random pppRNA sequence beyond the first nucleotide (GTP) appears to have no effect on the hydrolysis of 5′ phosphates. Uncatalyzed hydrolysis of random pppRNA and ATP (or GTP) in mildly acidic solution appears to proceed through a similar process, nucleophilic attack on the 5′ γ-phosphate by water, to produce P_i and ppRNA or ADP (or GDP).

On the other hand, catalysis by isolate 6 pppRNA in the presence of Ca^{2+} accelerates the overall hydrolysis rate 840-fold compared to uncatalyzed release of P_i by random pppRNA, and the hydrolysis cleavage pattern is also changed. Hydrolysis of isolate 6 pppRNA produces exclusively PP_i instead of P_i (Figure 3). Specific acceleration of PP_i release by isolate 6 pppRNA over random pppRNA is 170 000-fold. The specific cleavage pattern of isolate 6 pppRNA is probably linked to its cofactor Ca^{2+}, since PP_i is also released from ATP by hydrolysis in the presence of Ca^{2+} at pH 9 (Tetas & Lowenstein, 1963) and at pH 6.5 with the additional presence of 1,3-diaminopropane−cobalt complex (Tafesse & Milburrn, 1987), although in both cases P_i is also a hydrolysis product. Interestingly, there exist protein ATP pyrophosphohydrolases (producing PP_i and AMP) that also require Ca^{2+} for high specificity (Kawamura & Nagano, 1975; Flodgaard & Torp-Pedersen, 1978).

Although both random pppRNA and G(5′)pppRNA have three 5′ phosphates, capping equalizes the 5′ phosphate hydrolysis cleavage pattern and stabilizes the 5′ phosphates against hydrolysis. In contrast to random pppRNA where hydrolysis occurs predominantly between the 5′ β- and γ-phosphates (releasing P_i) in 2 mM Ca^{2+} and 20 mM MES (pH 5.5) (Figure 11), capped random G(5′)pppRNA hydrolyzes the 5′ phosphates almost randomly, producing P_i, GMP, GDP, and GTP with yields of the same order under the above conditions (Figure 12). This is, in part, the consequence of the chemical symmetry of the G(5′)pppG cap in the absence of an RNA tertiary structure. Overall, hydrolysis of random G(5′)pppRNA is 10 times slower than that of random pppRNA (1×10^{-5} min^{-1} vs 1×10^{-4} min^{-1}).

On the other hand, catalysis of hydrolysis by isolate 6 pppRNA and capped G(5′)pppRNA in the presence of Ca^{2+} results in the same high specificity (cleavage only between the 5′ α- and β-phosphates). Nevertheless, there are apparent differences between pyrophosphatase and decapping activities, although pyrophosphate release from isolate 6 pppRNA and the hydrolysis of GDP from the G(5′)pppRNA are similar reactions (reactions 2 and 3). First, capping makes the RNA less reactive. Capping slows down the hydrolysis (k_{cat}) about 5-fold (comparing pppRNA with G(5′)pppRNA) (Tables 1 and 2). Second, capping also increases (up to 9-fold) the Michaelis-Menten constant K_M for Ca^{2+}, which suggests looser binding of Ca^{2+} to G(5′)pppRNA than to pppRNA. Catalytic efficiency (k_{cat}/K_M) of isolate 6 RNA hydrolysis is also decreased (up to 50-fold) by capping due to both k_{cat} and K_M changes.

Among known ribozymes, isolate 6 RNA has a unique metal ion requirement for Ca^{2+} or Mn^{2+} ($Ca^{2+} > Mn^{2+}$). Most known ribozymes are metalloenzymes (Yarus, 1993; Pyle, 1993; Van Atta & Hecht, 1994), and the majority use Mg^{2+} as the activating metal ion. However, other metal ions can support catalytic activity or play essential structural roles (Table 3); for example, self-aminoacylationg RNAs also depend on Ca^{2+} in a unique role (e.g., Illangasekare et al., 1995). But among known ribozymes, isolate 6 RNA is rare in depending on either Ca^{2+} or Mn^{2+} as a sufficient ion, playing a structural and/or catalytic role that Mg^{2+} cannot fulfill.

This is unexpected because Mn^{2+} often replaces Mg^{2+} to activate both ribozymes (see Table 3) and protein enzymes (McEuen, 1982). Mutual interchangeability between Mn^{2+} and Mg^{2+} is explained as a result of similar size (0.72 vs 0.83 Å) (Shannon & Prewitt, 1969) and preferred coordination number of 6. On the other hand, Mn^{2+} and Ca^{2+} differ in these respects. Ca^{2+} has a large ionic radius of 1.00 Å (for 6-coordination, see Shannon & Prewitt (1969)), and its coordination number varies from 6 to 8 (Kaim & Schwederski, 1991). Thus, at least one essential metal site in this RNA has an unusual selectivity; for example, considering only ion radii (assuming 6-coordination), Mn^{2+} lies between Mg^{2+} and Ca^{2+} (closer to Mg^{2+} than to Ca^{2+}). Accordingly,

Table 3: Metal Ion Requirement of Some Ribozymes

ribozyme	required metal ion	ref
Tetrahemena group I intron	Mg^{2+} or Mn^{2+}	Cech and Bass, 1986; Grosshans & Cech, 1989
Tetrahemena ribozyme variant	Mg^{2+}, Ca^{2+}, or Mn^{2+}	Lehman & Joyce, 1993
hammerhead ribozyme	Mg^{2+}, Mn^{2+}, Ca^{2+} or Co^{2+} Zn^{2+}, Cd^{2+}, or Sr^{2+} + polyamine	Dahm & Uhlenbeck, 1991
human hepatitis delta virus	Mg^{2+}, Mn^{2+}, Ca^{2+} or Sr^{2+}	Suh et al., 1993
hairpin ribozyme	Mg^{2+}, Sr^{2+}, or Ca^{2+} Mn^{2+} or Co^{2+} + polyamine	Chowrira et al., 1993
Mn^{2+}-dependent hairpin ribozyme	Mn^{2+}, Cd^{2+}, Co^{2+}, or Cu^{2+}	Dange et al., 1990; Van Atta & Hecht, 1994
RNase P RNA	Mg^{2+} Mn^{2+} + polyamine	Guerrier-Takada et al., 1986

Table 4: Apparent Metal Ion-RNA Binding Constants $K_{1/2}$[a]

ribozyme	$K_{1/2}$	ref
Tetrahemena group I intron	~0.5 mM Mg^{2+}	Grosshans & Cech, 1989
group II intron ribozyme	~40 mM Mg^{2+}	Franzen et al., 1994
Hammerhead ribozyme	>3 mM Mg^{2+}, Mn^{2+}, and Ca^{2+} 5.3 mM Mg^{2+}	Dahm & Uhlenbeck, 1991 Perreault et al., 1991
human hepatitis delta virus (HDV)	≥0.3 mM Mg^{2+}, Mn^{2+}, Ca^{2+}, and Sr^{2+}	Suh et al., 1993
hairpin ribozyme	3 mM Mg^{2+}, 10 mM Sr^{2+}, 20 mM Ca^{2+}	Chowrira et al., 1993
RNase P RNA	36 mM Mg^{2+}	Beebe et al., 1996

[a] $K_{1/2}$ is defined as the concentration of metal ions giving half the maximum activity.

an essential site in isolate 6 RNA may be nonfunctional when occupied by too small an ion (Mg^{2+}) or one that is too large (Sr^{2+} or Ba^{2+}). Nevertheless, it is not obvious how a site of such specificity could be constructed within an RNA structure.

Isolate 6 RNA not only requires Ca^{2+} for activity but also probably binds Ca^{2+} strongly at pH > 7, as indicated by a low K_M of 40−60 μM for Ca−pppRNA and 100−200 μM for Ca−G(5′)pppRNA complexes. For an enzyme reaction following the general mechanism

$$S + E \underset{k_{-1}}{\overset{k_1}{\rightleftharpoons}} ES \xrightarrow{k_p} P \qquad (14)$$

it follows that

$$K_M = (k_{-1} + k_p)/k_1 = k_{-1}/k_1 + k_p/k_1 = K_d + k_p/k_1 \qquad (15)$$

$$K_d \leq K_M \qquad (16)$$

Thus, in any mechansim having a single Michaelis complex (ES) between a substrate and product(s), dissociation constant (K_d) of a substrate−enzyme complex or an activator−enzyme complex is equal to or smaller than K_M. Under these assumptions, K_d of the Ca−pppRNA complex is at most 40−60 μM. This is among the strongest divalent metal ion affinity for RNA catalysts known (Table 4), although similar divalent dissociation determined by physical methods have been reported. There are weak and strong metal sites with K_d of 1 and 0.01 mM, respectively, in tRNA (Van Atta & Hecht, 1994) and ~0.1 mM Mg^{2+} in the hammerhead ribozyme (Koizumi & Ohtsuka, 1991). Ca^{2+}-binding constant by isolate 6 RNA compares well to many Ca^{2+}-dependent metalloproteins (Strynadka & James, 1989), for example, bovine β-trypsin, 0.4 mM; thermolysin, 20 μM; phospholipase A_2, 0.25 mM; staphylococcal nuclease, ~1 mM; concanavalin A, 0.3 mM; bovine calmodulin, ~10 μM; avian troponin C, ~10 μM.

The three catalytic activities of isolate 6 RNA can be summarized as two competing reactions

$$Rppp\mathbf{p}RNA + H_2O \xrightarrow{k_{H_2O}} Rpp + \mathbf{p}RNA \qquad (17)$$

$$Rppp\mathbf{p}RNA + Nu \xrightarrow{k_{Nu}} Rpp + Nu\text{-}\mathbf{p}RNA \qquad (18)$$

where R can be absent or a nucleoside or a nucleotide and Nu can be virtually any nucleophile with an unblocked terminal phosphate (Huang & Yarus, 1976b). Reactions 17 (hydrolysis) and 18 (capping or cap exchange) are not independent. Instead, they are related by:

$$k_{H_2O} + k_{Nu} = \text{constant under given pH and calcium concentration}$$

This explains several otherwise anomalous observations. We have shown previously that the self-capping from 1 mM GDP and pyrophosphate release (no GDP present) of the pppRNA have about the same rates in the selection buffer, and yet the capping yield is high, approaching 70% within 1 h (Huang & Yarus, 1977a).

In the presence of GDP, the pppRNA undergoes GDP-dependent self-capping and water-dependent pyrophosphate release simultaneously. Because GDP does not change the overall pyrophosphate release by the pppRNA (Figure 6), the pyrophosphatase activity is decreased in the presence of GDP. Therefore, isolate 6 pppRNA can be capped to high yield with an external nucleophile.

The inhibition of G(5′)pppRNA decapping by GDP (at >1 μM) or ppppG is also explained by a constant rate for the overall disappearance of the G(5′)pppRNA. Decapping of the G(5′)pppRNA to the pRNA decreases 8- to 9-fold with ppppG present, and simultaneously ~90% of the starting G(5′)pppRNA is converted to G(5′)ppppRNA. The inhibition of decapping of G(5′)pppRNA to pRNA by 1 mM ppppG is about the same as that by 1 mM GDP (90−95% reduction). Thus, in the presence of a terminal phosphate-containing nucleophile, water and the nucleophile compete, maintaining a constant overall reaction rate determined by the pH, temperature, and Ca^{2+} concentration.

On the basis of hydrolysis studies for NTPs from the literature, we suggest a two-calcium model for this RNA. One calcium bridges the nucleophilic attacking group and the 5′ α-phosphate and the other calcium bridges the (*β*, *γ*)-phosphates. Such a model can explain the high specificity and an inverse relationship between pyrophosphatase and capping activities.

(1) The reaction is centered at the 5′ α-phosphate of the pppRNA, so Ca^{2+} binding likely involves the 5′ phosphates. (2) The K_M (Table 1) of the pppRNA is close to the apparent K_d of CaATP, and the pH dependence of K_M parallels the pH dependence of the apparent K_d of CaATP complex (3, 0.2, and 0.1 mM at pH 5.5, 7.0, and 8.5, respectively; Nanninga, 1961), indicating that a catalytically important Ca^{2+} is indeed coordinated by the 5′ phosphates. (3) Capping the 5′ end reduces K_M up to 9-fold (Tables 1 and 2), strongly suggesting direct interaction of Ca^{2+} with the 5′ phosphates. (4) Hydrolysis studies of M^{2+}−NTPs have established the 2:1 M^{2+}:NTP complex as the reactive species (Sigel, 1990). (5) Coordination of M−α,*β*-phosphates and M(OH)−*γ*-phosphate of NTPs leads to cleavage between *β*- and *γ*-phosphates (producing P_i) resulting from nucleophilic attack on the *γ*-phosphate by the metal-coordinated nucleophile OH group (Sigel, 1990). To account for the unique production of PP_i, we suggest that the coordination pattern is changed to Ca−*β*,*γ*-phosphates and Ca(Nu)−α-phosphate (Nu = nucleophilic attacking group) through the intervention of the tertiary structure of isolate 6 pppRNA.

In this model, the Ca^{2+} complexing with the *β*,*γ*-phosphates helps to position and orient the α-phosphate and reduce the overall negative charge on the phosphates so as to facilitate nucleophilic attack. The other Ca^{2+} plays dual roles of coordinating the nucleophilic attacking group to aid attack on the α-phosphate and stabilizing the transition state through coordination of the phosphate oxygens. Because the attacking group is coordinated to the Ca^{2+} that binds to the phosphate, the reaction is centered only at the α-phosphate. Different nucleophiles bind competitively to this Ca^{2+}, which produces competition between the hydrolysis and capping or cap-exchange. Thus far, the model does not specifically predict a constant total rate of reaction. A constant rate implies, in addition, a common conformational or chemical rate-determining step for reaction with both water and nucleophiles.

The two-Ca^{2+} model also does not specify the kinetically-defined Ca^{2+}-binding site. Lineweaver−Burk plots do not reveal cooperativity (non−linearity). Thus, the binding affinity of the two Ca^{2+} sites may differ by more than 1 order of magnitude, so that the activity would respond hyperbolically to the last-bound essential Ca^{2+} (at the weaker site).

Finally, we suggest a specific application of the unusual versatility of isolate 6, the creation of combinatorial ribozymes. On one hand, many different kinds of small-molecule (that is, substrate) binding sites can be folded from pure RNA (Yarus, 1988; Connell et al., 1993; Majerfeld & Yarus, 1994; Ellington & Szostak, 1990; Sassanfar & Szostak, 1993; Lorsch & Szostak, 1994). On the other hand, isolate 6 RNA is a stable, independent structure containing an active center that labilizes the 5′ α phosphate of the RNA to attack by several nucleophiles, including at least HOH (water) and mono-, di-, tri-, and tetraphosphate oxygens, and the latter may be a part of nucleotides, amino acids, sugars, or other RNAs (Huang & Yarus, 1997b).

Secondly, RNA can oligomerize accurately with little cost in information. A short oligomerization tract of as few as five or six nucleotides might be used to join a reaction center such as that of isolate 6 to binding centers for several substrates. This process could create differing substrate-specific enzymes carrying out similar reactions. That is, isolate 6 employs the same active center to become a pyrophosphatase and a capping and decapping catalyst—might a related RNA serve as a subunit for an RNA replicase, which catalyzes ROH attack on the 5′ α phosphate of nucleotides? This process is particularly appealing for RNAs with kinetics like isolate 6, which has a constant rate of total reaction. The redirection of its reactivity to a new substrate would thereby minimize side reactions (e.g., hydrolysis) and result in a highly specific new activity.

However, we can think of several deficiencies that might be manifested in ribozymes made of interchangeable active center and substrate-binding domains. For example, a combinatorial ribozyme composed of several subunits could be flexible and thereby inferior in catalytic accuracy and rate acceleration to a unified one.

There is much evidence that such difficulties are not limiting, even when ribozymes are assembled from pieces chosen for experimental motives, rather than being evolved for optimal function. A highly active group I self-splicing RNA has been assembled from as many as four fragments (Doudna et al., 1991) that combine by a mixture of base pairing and tertiary interactions, and a quite different three-fragment group I ribozyme held together largely by tertiary forces is also active (Doudna and Cech, 1995). A partial reaction of group II self-splicing is accurately carried out by a three-RNA assembly whose two catalytic domains combine by tertiary forces alone (Franzen et al., 1993; Michels & Pyle, 1995).

Clearly, the reuse of optimal catalytic motifs is a frequent adaptive theme in protein enzymes. We can therefore envision that facile RNA oligomerization could create a combinatorial ribozyme consisting of an isolate 6-like catalytic subunit and substrate binding subunit(s) that self-assemble into quaternary structures. Such a combinatorial strategy would be economical of primordial coded information at a time when such information and its expression might have been costly.

ACKNOWLEDGMENT

We thank the members of our lab for comments on a draft manuscript.

REFERENCES

Beebe, J. A., Kurz, J. C., & Fierke, C. A. (1996) *Biochemistry 35*, 10493.

Beelman, C. A., Stevens, A., Caponigro, G., LaGrandeur, T. E., Hatfield, L., Fortner, D. M., & Parker, R. (1996) *Nature 382*, 642.

Cech, T. R., & Bass, B. L. (1986) *Annu. Rev. Biochem. 55*, 599.

Chowrira, B. M., Berzal-Herranz, A., & Burke, J. M. (1993) *Biochemistry 32*, 1088.

Connell, G. J., Illangesekare, M., & Yarus, M. (1993) *Biochemistry 32*, 5497.

Dahm, S. C., & Uhlenbeck, O. C. (1991) *Biochemistry 30*, 9464.

Dange, V., Van Atta, R. B., & Hecht, S. M. (1990) *Science*, *248*, 585.

Decker, C. J., & Parker, R. (1993) *Genes Dev. 7*, 1632.
Decker, C. J., & Parker, R. (1994) *Trends Biochem. Sci. 19*, 336.
Doudna, J. A., & Cech, T. R. (1995) *RNA 1*, 36.
Doudna, J. A., Couture, S., & Szostak, J. W. (1991) *Science 251*, 1605.
Ellington, A. D., & Szostak, J. W. (1990) *Nature 346*, 818.
Flodgaard, H., & Torp-Pedersen, C. (1978) *Biochem. J. 171*, 817.
Franzen, J. F., Zhang, M., & Peebles, C. L. (1993) *Nucleic Acid Res. 21*, 627.
Franzen, J. S., Zhang, M., Chay, T. R., & Peebles, C. L. (1994) *Biochemistry 33*, 11315.
Gilbert, W. (1986) *Nature 319*, 618.
Grosshans, C. A., & Cech, T. R. (1989) *Biochemistry 28*, 6888.
Guerrier-Takada, C., Haydock, K., Allen, L., & Altman, S. (1986) *Biochemistry 25*, 1509.
Hock, A., & Huber, G. (1956) *Biochem. Z. 328*, 44.
Huang, F., & Yarus, M. (1997a) *Biochemistry 36*, 6557.
Huang, F., & Yarus, M. (1997b) *Proc. Natl. Acad. Sci. U.S.A. 94*, 8965.
Hubner, P. W. A., & Milburrn, R. M. (1980) *Inorg. Chem. 19*, 1267.
Hulett, H. R. (1970) *Nature 225*, 1248.
Illangasekare, M., Sanchez, G., Nickles, T., & Yarus, M. (1995) *Science 267*, 643.
Joyce, G. F. (1989) *Nature 338*, 217.
Kaim, W., & Schwederski, B. (1991) *Bioinorganic Chemistry: Inorganic Elements in the Chemistry of Life*, John Wiley & Sons.
Kawamura, M., & Nagano, K. (1975) *Biochim. Biophys. Acta 397*, 207.
Koizumi, M., & Ohtsuka, E. (1991) *Biochemistry 30*, 5145.
Lehman, N., & Joyce, G. F. (1993) *Nature 361*, 182.
Liebecq, C., & Jacquemotte-Louis, M. (1958) *Bull. Soc. Chim. Biol. 40*, 67.
Lorsch, J. R., & Szostak, J. W. (1994) *Biochemistry 33*, 973.
Majerfeld, I., & Yarus, M. (1994) *Nature Struct. Biol. 1*, 287.
McEuen, A. R. (1982) in *Inorganic Biochemistry vol. 3* (Hill, H. A. O., Ed.) pp. 314, Royal Society of Chemistry, London.
Michels, W. J., & Pyle, A. M. (1995) *Biochemistry 34*, 2965.
Muhlrad, D., Decker, C. J., & Parker, R. (1994) *Genes Dev. 8*, 855.
Muhlrad, D., Decker, C. J., & Parker, R. (1995) *Mol. Cell. Biol. 15*, 2145.
Nanninga, L. B. (1961) *Biochim. Biophys. Acta 54*, 330.
Perreault, J. P., Labuda, D. Usman, N., Yang, J. H., & Cedergren, R. (1991) *Biochemistry 30*, 4020.
Pyle, A. M. (1993) *Science 261*, 709.
Sassanfar, M., & Szostak, J. W. (1993) *Nature 364*, 550.
Shannon, R. D., & Prewitt, C. T. (1969) *Acta Crystallogr. B25*, 925.
Sigel, H. (1990) *Coord. Chem. Rev. 100*, 453.
Sigel, H., & Hofstetter, F. (1983) *Eur. J. Biochem. 132*, 569.
Stevens, A. (1980) *Biochem. Biophys. Res. Commun. 96*, 1150.
Strynadka, N. C. J., & James, M. N. G. (1989) *Annu. Rev. Biochem. 58*, 951.
Suh, Y. A., Kumar, P. K., Taira, K., & Nishikawa, S. (1993) *Nucleic Acids Res. 21*, 3277.
Tetas, A., & Lowenstein, J. M. (1963) *Biochemistry 2*, 350.
Tafesse, F., & Milburrn, R. M. (1987) *Inorg. Chim. Acta 135*, 119.
Van Atta, R. B., & Hecht, S. M. (1994) *Adv. Inorg. Biochem. 9*, 1 (and references therein).
White, H. B. (1976) *J. Mol. Biol. 7*, 101.
Yarus, M. (1993) *FASEB J. 7*, 31.

BI971081N